Energetics of *S*-Adenosylmethionine Synthetase Catalysis†

Michael S. McQueney,‡,§ Karen S. Anderson,‖ and George D. Markham*,‡

Institute for Cancer Research, Fox Chase Cancer Center, 7701 Burholme Avenue, Philadelphia, Pennsylvania 19111, and Department of Pharmacology, Yale University, New Haven, Connecticut 06520

Received December 15, 1999; Revised Manuscript Received February 10, 2000

ABSTRACT: *S*-Adenosylmethionine synthetase (ATP:L-methionine *S*-adenosyltransferase) catalyzes the only known route of biosynthesis of the primary biological alkylating agent. The internal thermodynamics of the *Escherichia coli S*-adenosylmethionine (AdoMet) synthetase catalyzed formation of AdoMet, pyrophosphate (PP_i), and phosphate (P_i) from ATP, methionine, and water have been determined by a combination of pre-steady-state kinetics, solvent isotope incorporation, and equilibrium binding measurements in conjunction with computer modeling. These studies provided the rate constants for substrate binding, the two chemical interconversion steps [AdoMet formation and subsequent tripolyphosphate (PPP_i) hydrolysis], and product release. The data demonstrate the presence of a kinetically significant isomerization of the E·AdoMet·PP_i·P_i complex before product release. The free energy profile for the enzyme-catalyzed reaction under physiological conditions has been constructed using these experimental values and in vivo concentrations of substrates and products. The free energy profile reveals that the AdoMet formation reaction, which has an equilibrium constant of 10^4, does not have well-balanced transition state and ground state energies. In contrast, the subsequent PPP_i hydrolytic reaction is energetically better balanced. The thermodynamic profile indicates the use of binding energies for catalysis of AdoMet formation and the necessity for subsequent PPP_i hydrolysis to allow enzyme turnover. Crystallographic studies have shown that a mobile protein loop gates access to the active site. The present kinetic studies indicate that this loop movement is rapid with respect to k_{cat} and with respect to substrate binding at physiological concentrations. The uniformly slow binding rates of 10^4-10^5 M^{-1} s^{-1} for ligands with different structures suggest that loop movement may be an intrinsic property of the protein rather than being ligand induced.

S-Adenosylmethionine synthetase (ATP:L-methionine *S*-adenosyltransferase) is an ubiquitous enzyme that catalyzes the formation of AdoMet, the primary biological alkylating agent (*1*−*4*). AdoMet is the major methyl group donor in biological systems, being used in the methylation of proteins, small molecules, RNA, and DNA (*5*−*8*). In addition, AdoMet also serves as a source of the propylamine moiety in spermine and spermidine biosynthesis (*9*, *10*) and as a free radical progenitor in several enzymatic reactions (*11*). AdoMet is a precursor of the acyl-homoserine lactones used by some bacteria in sensing cell density (quorum sensing) (*12*) and of the plant growth hormone ethylene (*13*).

AdoMet synthetase catalyzes the two sequential reactions:

$$\mathrm{ATP + Met \rightarrow \underset{\text{enzyme bound}}{[AdoMet + PPP_i]} + H_2O \rightarrow AdoMet + PP_i + P_i}$$

In the first step, the sulfur of methionine attacks the C5′ of ATP, producing enzyme-bound AdoMet and PPP_i[1] (*14*, *15*); stereochemical and kinetic isotope effect studies show that this reaction occurs in a S_N2 mechanism (*16*, *17*). In the second reaction, the enzyme-bound PPP_i is hydrolyzed to PP_i and P_i, both of which are released from the enzyme prior to AdoMet dissociation; >98% of the P_i formed originates from the γ-phosphoryl group of ATP showing that bound PPP_i does not readily reorient in the active site (*14*, *15*). Kinetic isotope effect measurements with the *Escherichia coli* enzyme, the isoform that has been studied in the most detail (*15*, *17*−*25*), show that the reaction forming AdoMet and PPP_i is the rate-limiting step up to the first irreversible step in the reaction pathway, which also appears to be AdoMet formation. The equilibrium for the overall reaction favors product formation, minimally due to the involvement of water as a reactant (*14*). A detailed analysis of the kinetics of the reaction pathway and of the interconversion of the central complexes has not been reported previously.

The crystallographic structure of the *E. coli* enzyme, a tetramer of 383 residue subunits, shows the presence of a 13-residue loop that is positioned to act as a gate to the active site; the position of this loop varies in the presence or absence of ligands (*23*−*25*). Interestingly, this loop is the least conserved internal segment in a protein that is highly conserved through eukarya and prokarya (e.g., 54% amino

† This research was supported by NIH Grants GM31186 (to G.D.M.), AI44630 (to K.S.A.), and CA06927 (to FCCC) and was also supported by an appropriation from the Commonwealth of Pennsylvania. The contents of this paper are solely the responsibility of the authors and do not necessarily represent the official views of the National Cancer Institute or any other sponsoring organization.

* To whom correspondence should be addressed. Tel: 215-728-2439. Fax: 215-728-3574. E-mail: GD_Markham@fccc.edu.

‡ Fox Chase Cancer Center.

§ Present address: Department of Protein Biochemistry, SmithKline Beecham, King of Prussia, PA.

‖ Yale University.

[1] Abbreviations: PPP_i, tripolyphosphate; K_t, concentration of the second substrate (S2) producing half-maximal trapping of the first substrate (S1) when S2 binds to the E·S1 complex.

[2] R. S. Reczkowski and G. D. Markham, unpublished results.

10.1021/bi992876s CCC: $19.00
Published on Web 03/25/2000

acid identity over the entire sequence between the *E. coli* and human enzymes). Interestingly, the k_{cat} values of the isoforms vary by as much as 100-fold although the active site residues are all conserved; the *E. coli* enzyme has the highest turnover number of any characterized AdoMet synthetase. The requirement of a protein isomerization, perhaps a loop movement, for substrate binding is consistent with the low k_{cat}/K_m values of 10^4-10^5 M^{-1} s^{-1} for each substrate (*15*).

Pre-steady-state kinetics and isotope partitioning experiments have become invaluable tools in elucidating the internal workings of enzymes (*26*−*30*). The present work has used stopped-flow and rapid-quench kinetic studies, in combination with isotope trapping and solvent isotope incorporation methods, equilibrium binding experiments, and computer modeling, to determine the rate constants for each step in the interconversion of substrates to products. These studies reveal the presence of a previously veiled isomerization along the reaction pathway. The free energy profile for the enzyme-catalyzed reaction at physiological concentrations of substrate and product has been constructed using these kinetic constants in conjunction with reported in vivo concentrations of ATP, methionine, AdoMet, PP_i, and P_i. In addition to aiding in understanding the catalytic proficiency of the enzyme, the results provide insight into the dynamic properties of the enzyme's active site gate.

MATERIALS AND METHODS

General. [8-^{14}C]ATP (58.9 mCi/mmol), [γ-^{32}P]ATP (30 Ci/mmol), [*methyl*-^{14}C]-L-methionine (55 mCi/mmol), $^{32}PP_i$ (19 Ci/mmol), and $^{32}P_i$ (200 Ci/mmol) were purchased from Dupont−NEN. ATP, methionine, PPP_i, PP_i, P_i, and other reagents were purchased from Sigma. PEI−cellulose thin-layer plates were obtained from EM Scientific. L-*cis*-1-Amino-4-methoxybutenoic acid (cis-AMB) was a gift from Dr. Janice Sufrin, Roswell Park (*31*). AdoMet was purchased from RBI and purified by ion-exchange chromatography before use (*32*). *E. coli* AdoMet synthetase was purified as previously described (*15*, *20*). Enzyme concentrations were determined from the absorbance at A_{280} (an A_{280} of 1.3 reflects a 1.0 mg/mL solution of the enzyme) (*15*). The subunit mass of 42 kDa was used to calculate enzyme active site concentration. Experiments were conducted at 25 °C in 50 mM Hepes−KOH, 50 mM KCl, 20 mM $MgCl_2$, and 10% glycerol, pH 8.0, unless otherwise noted; 10% glycerol did not alter the k_{cat}.

$^{32}PPP_i$ was prepared from [^{32}P]ATP by periodate oxidation followed by aniline cleavage of the sugar−phosphate linkage (*33*). All steps were performed at room temperature. Twenty microliters of 0.5 M $NaIO_4$ was added to a 400 μL solution of 9 mM [^{32}P]ATP (45 mCi/mmol). After 80 min at room temperature, 100 μL of ethylene glycol was added to consume excess periodate. After 15 min, 1 mL of 1 M aniline adjusted to pH 5 with HCl was added. After 2 h, 10 mg of Norit was added, and after thorough mixing the solution was clarified by centrifugation. $^{32}PPP_i$ was purified by ion-exchange chromatography on QAE-A25 Sephadex; after being loaded, the resin was washed with 3 volumes of water, and $^{32}PPP_i$ was eluted with 1 M triethylamine bicarbonate, pH 7.5. The $^{32}PPP_i$ was lyophilized to dryness, followed by two cycles of drying from methanol. The resulting compound was radiochemically pure as judged by thin-layer chromatography on PEI−cellulose sheets.

Fluorescence Titration Measurements. Equilibrium fluorescence experiments were carried out by monitoring changes in intrinsic protein fluorescence using a Perkin-Elmer LS-50 luminescence spectrophotometer. The excitation wavelength was typically 295 nm, and fluorescence emission spectra (310−400 nm) were obtained as an average of three scans. The decrease in fluorescence due to substrate/product binding was monitored at 333−345 nm. A typical experiment involved the titration of a 2 mL solution of AdoMet synthetase (0.04 μM active sites) with microliter aliquots of ligand. The observed data were corrected for dilution and plotted versus total ligand concentration. The data were then fit to eq 1 by nonlinear regression using the program Enzfitter

$$F = -T[L/(L + K_d)] + M \quad (1)$$

(Elsevier Biosoft). The dissociation constant (K_d) and total fluorescence change in formation of the complex were calculated using the observed change in fluorescence (F), the total fluorescence in the absence of ligand (M), the extent of fluorescence quenching at a saturating ligand concentration (T), and the concentration of ligand (L). Inner filter effects complicated analyses of the titration of AdoMet synthetase with ATP and AdoMet. The data were corrected for inner filter effects using the graphical extrapolation method described by Mertens and Kägi (*34*, *35*).

In ATP binding experiments the nucleotide concentration ranged from 0.01 to 2 mM. In methionine binding experiments the ligand concentration ranged from 0.01 to 5 mM. In studies of binding to binary enzyme−ligand complexes, the ATP concentration was 12 mM for experiments monitoring methionine binding, and the methionine concentration was 15 mM when ATP binding was measured.

Affinity of P_i for the E·AdoMet·PP_i Complex. The affinity of P_i was determined by measuring the amount of radiolabeled PPP_i formed from $^{32}PP_i$ and P_i. Since the affinity of AdoMet synthetase for P_i is low [as indicated by K_i values of 8−25 mM for noncompetitive inhibition of AdoMet formation (*15*)], the formation of PPP_i was measured when various amounts of P_i were added to solutions (25 μL) containing 1.7 mM enzyme active sites, 1 mM AdoMet, and 0.25 mM $^{32}PP_i$ (28 mCi/mmol), conditions in which >90% of the PP_i would be enzyme bound. After a 30 s incubation, 5 μL of 25% trichloroacetic acid containing 1 mM PPP_i and 1 mM PP_i was added. Samples (5 μL) were spotted on PEI−cellulose F plates and allowed to air-dry. The plates were soaked for 15 min in CH_3OH, air-dried, and chromatographed in 1.8 M LiCl, 50 mM EDTA, pH 6. R_f values were 0.78 for P_i, 0.32 for PP_i, and 0.16 for PPP_i. Radioactive compounds were visualized by autoradiography, spots were then cut out, and radioactivity was quantified by scintillation counting.

Substrate Trapping by Pulse−Chase Experiments. Pulse−chase experiments were performed to determine the partitioning of enzyme-bound substrates between product formation and dissociation (*36*, *37*). A solution of AdoMet synthetase and a ^{14}C-labeled substrate (the pulse) was mixed with a solution of a large molar excess of unlabeled substrate and cosubstrate (the chase) in a KinTek RQF-3 rapid-quench apparatus. At various times the reactions were terminated

by mixing with 190 μL of 0.6 N HCl and 50 mM Hepes. The acid-quenched reactions were then adjusted to pH 6−7 by addition of 10 N KOH. Protein was precipitated by the addition of 50 μL of CCl_4 followed by vigorous vortexing. After centrifugation, 25 μL of the supernatant was spotted on a 2 cm diameter disk of Whatman P81 filter paper. After air-drying, the filter papers were washed with 4 L of distilled water. The disks were then placed in vials with scintillation cocktail (Ecoscint) and analyzed by liquid scintillation counting. In control experiments the labeled substrate was included in the syringe with the unlabeled substrate rather than with the enzyme.

The pulse solution for the ATP trapping experiment contained 0.6 mM [8-^{14}C]ATP (58.9 mCi/mmol) and 0.1 mM AdoMet synthetase (concentrations before mixing). The chase contained 44 mM ATP, 44 mM $MgCl_2$, and 14 mM methionine. The pulse solution for the methionine trapping experiment contained 0.6 mM [*methyl*-^{14}C]methionine (55 mCi/mmol) and 0.1 mM AdoMet synthetase; the chase solution contained 44 mM methionine, 14 mM ATP, and 14 mM $MgCl_2$.

Determination of the Dissociation Rate (k_{off}) of ATP. The pulse−chase experiment was carried out by mixing a solution of 0.1 mM [8-^{14}C]ATP (58.9 mCi/mmol) and 0.2 mM AdoMet synthetase with a solution containing 0.2−100 mM methionine and 28 mM ATP (the chase) and incubating for 10 s. The reactions were terminated by addition of 190 μL of 0.6 N HCl and Hepes−KOH (50 mM). KOH (10 M) was then added to adjust the pH to 6−7. The protein was precipitated by addition of 50 μL of CCl_4, followed by vigorous vortexing. Aliquots (25 μL) of the supernatants were spotted on a 2 cm disk of P81 filter paper. After air-drying the disks were placed in a Büchner funnel, washed with 4 L of distilled water, and put into 5 mL tubes with scintillation cocktail (Ecoscint) and analyzed by liquid scintillation counting.

Stopped-Flow Fluorescence Experiments. Stopped-flow experiments were carried out using a KinTek stopped-flow SF-2001 apparatus. A 0.5 cm path-length cell was used. Ligand binding to the enzyme was followed by monitoring changes in intrinsic enzyme fluorescence; fluorescence was excited at 290 nm, and emission was monitored at 330 nm. In most experiments an average of four shots was used for data analysis. All experiments used 2.5 μM AdoMet synthetase active sites. At least a 5-fold excess of variable ligand over enzyme was present to allow analysis of the observed rate constant, k_{obsd}, as a pseudo-first-order rate constant. The observed rate constants were obtained by fitting the data to a single exponential using a nonlinear least-squares program. When a linear dependence of k_{obsd} on ligand concentration was apparent, the observed rate constants were fit to the equation

$$k_{obsd} = k_{on}[\text{ligand}] + k_{off} \quad (2)$$

in order to obtain the ligand binding rate constant and in favorable cases an estimate of the dissociation rate constant (*27*). The concentration dependence for PPP_i binding was nonlinear, and the analysis of those data is described in the Results section.

Rate of P_i Binding. The rate of P_i binding was determined from the rate of PPP_i formation under conditions where the reaction rate was limited by the second-order rate of P_i association. A solution of AdoMet synthetase, PP_i, and AdoMet was mixed with a solution of PP_i, AdoMet, and $^{32}P_i$ in the rapid-quench apparatus. The concentrations of reactants after mixing were 50 μM AdoMet synthetase, 4 μM $^{32}P_i$ (200 Ci/mmol), 4 mM PP_i, and 1 mM AdoMet. At various times the reactions were quenched with 0.6 N KOH and then neutralized with HCl. Compounds were separated by TLC on PEI−cellulose sheets developed in 1.3 M LiCl, 50 mM EDTA, pH 6, and quantified by detection on an AMBIS two-dimensional radioactivity detector.

Rate of Reversal of the AdoMet Synthetase Reaction. The rate of the reverse AdoMet synthetase reaction was determined by monitoring the time course (0.5 min to 5 h) of [^{32}P]ATP formation from 2.1 mM AdoMet, 1.4 mM $^{32}PP_i$ (10 Ci/mmol), 100 mM P_i, and 1.5 mM AdoMet synthetase active sites. Aliquots (5 μL) of the reaction mixture were quenched with 5 μL of 25% TCA containing 1 mM ATP. After centrifugation the components in the acidic supernatant were separated by two-dimensional TLC on 5 × 5 cm PEI−cellulose plates, which was required due to the small amounts of product formed. The solvent systems described by Bochner and Ames were employed (*38*). The first dimension used solvent F_a (4 M formic acid adjusted to pH 4.5 with NH_4OH) in which ATP, PP_i, and PPP_i have R_f values of 0.35, <0.05, and <0.05, respectively. After the plates were air-dried, the second dimension was developed in solvent S_b [74 g of $(NH_4)_2SO_4$, 0.4 g of $(NH_4)HSO_4$, 4 g of Na_2EDTA, 100 mL of H_2O] in which ATP, PP_i, and PPP_i have R_f values of 0.45, >0.9, and >0.9, respectively. Compounds were visualized by autoradiography, the spots were then cut out, and radioactivity was quantified by scintillation counting.

^{18}O Incorporation from $H_2{}^{18}O$ into P_i. The stoichiometry of incorporation of solvent oxygen into the P_i formed in various AdoMet synthetase catalyzed reactions was assessed by carrying out reactions in 22% $H_2{}^{18}O$. The incorporation of ^{18}O into P_i was determined by ^{31}P NMR at 121 MHz (7 T), monitoring the −0.0206 ppm change in the chemical shift of P_i that accompanies ^{16}O replacement by ^{18}O (*39*). Spectra were digitized at a resolution of 0.125 Hz/point and processed using a Gaussian line broadening of 0.1 Hz. The overall AdoMet synthetase reaction was studied using 5.5 mM ATP and 5.5 mM methionine. The tripolyphosphate hydrolysis reaction was studied using 5.5 mM PPP_i in the presence and absence of 1 mM AdoMet. Solutions contained 10% D_2O for field-frequency locking.

Single Turnover Experiments. Single turnover reactions were carried out by mixing 46 μL of enzyme solution with 46 μL of a solution containing substrate(s), either [γ-^{32}P]ATP and methionine, $^{32}PPP_i$ and AdoMet, or $^{32}PP_i$, P_i, and AdoMet, in the rapid quench instrument. All solutions contained 50 mM Hepes−KOH, 50 mM KCl, 10% glycerol, and 20 mM $MgCl_2$. After a variable incubation period, the reactions were quenched by mixing with 190 μL of 0.6 N HCl. The reaction products were then adjusted to pH 7.5 ± 0.5 with KOH. Next, CCl_4 (50 μL) was added and the mixture vortexed to precipitate the protein. After centrifugation, the supernatant was removed for product analysis.

Radiolabeled compounds derived from the reactions were separated by thin-layer chromatography on PEI−cellulose F sheets. Samples (2 μL) were spotted on the plates and allowed to air-dry. The plates were soaked for 15 min in

Scheme 1: Reaction Sequence for AdoMet Synthetase Deduced from Steady-State Kinetic Measurements[a]

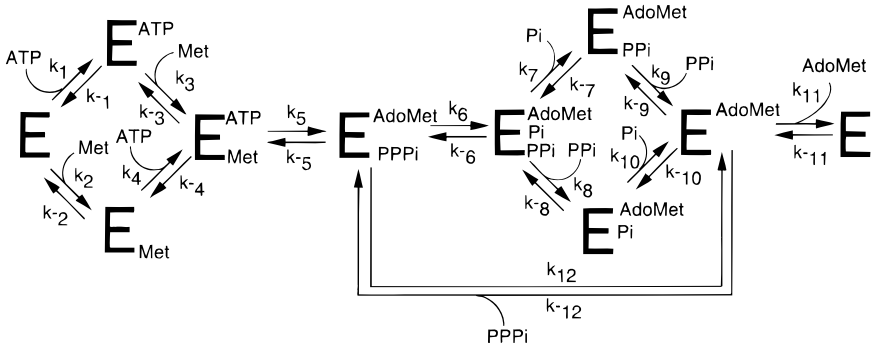

[a] See ref 15. The rate constants are labeled as they are referenced throughout the text.

Scheme 2: Reaction Sequence for AdoMet Synthetase Deduced from the Combination of Pre-Steady-State and Steady-State Kinetic Measurements[a]

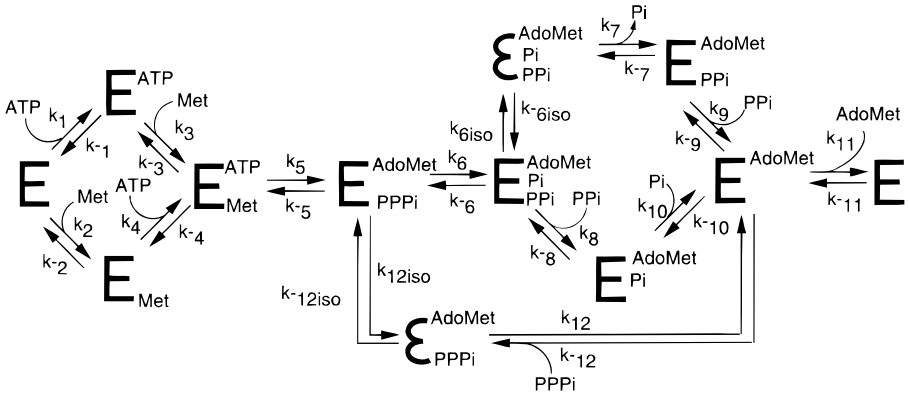

[a] The rate constants are labeled as they are referenced throughout the text. The addition steps found in this study are noted as $k_{\#,iso}$, where the number (#) is that of the preceding step in the sequence (Scheme 1). The isomerized E·AdoMet·PP_i·P_i and E·AdoMet·PPP_i complexes are shown in a different font.

CH_3OH, air-dried, and chromatographed in 0.9 M LiCl, 50 mM EDTA, pH 6. The radioactive spots were quantified using an AMBIS two-dimensional direct radiation detector.

Kinetic Modeling. The time courses for single turnover reactions of AdoMet synthesis, PPP_i hydrolysis, and the reverse reaction of PPP_i synthesis were fit to a computer model for the entire AdoMet synthetase reaction sequence using the programs KINSIM and FITSIM (*40*−*42*), as incorporated into the comprehensive KinTekSim program (KinTek Inc., http://www.kintec-corp.com). This modeling allowed refinement of experimentally determined rate constants into an internally consistent set of rate constants that describe the major reaction pathway.

RESULTS

Overview of the Methodology

The free energy profile for AdoMet synthetase was constructed by determining the rate constants in the forward and reverse directions for the individual steps in the mechanism that had been deduced from steady-state kinetic measurements (Scheme 1). Initially, the equilibrium constants for substrate and product binding were determined. Then the partitioning of the ternary E·ATP·Met complex between substrate dissociation and product formation was determined by pulse−chase experiments. Next, rate constants for substrate and product binding and/or dissociation were measured by stopped-flow fluorescence measurements or deduced from substrate trapping experiments. When only a single rate constant for a step was determined, the rate constant for the opposite direction was calculated using the equilibrium constant and the measured rate constant. The possible reversal of the hydrolytic reaction before product dissociation was assessed from the quantity of incorporation of ^{18}O from $H_2{}^{18}O$ into the P_i formed. Finally, single turnover experiments were carried out in the forward direction for the overall reaction

$$ATP + Met \leftrightarrows AdoMet + PPP_i \leftrightarrows AdoMet + PP_i + P_i$$

and for forward and reverse directions for the hydrolysis of added PPP_i

$$PPP_i + H_2O \leftrightarrows PP_i + P_i$$

The data revealed the presence of additional species beyond those shown in Scheme 1, and a more complete scheme was constructed (Scheme 2). The measured rate constants were used in the kinetic mechanism of Scheme 2 to simulate the time course of the single turnover data using the kinetic modeling programs KINSIM and FITSIM (*40*−*42*). The fitting process yielded refined internally consistent rate constants which were used in conjunction with published values of in vivo concentrations of ATP, methionine, AdoMet, PP_i, and P_i to construct the free energy profile of the AdoMet synthetase catalyzed reaction under physiological conditions.

Table 1: Equilibrium Constants for Ligand Binding to AdoMet Synthetase[a]

interaction	parameter	dissociation constant (mM)
ATP binding to E	K_1	1.4
methionine binding to E	K_2	0.58
methionine binding to E·ATP	K_3	0.025
ATP binding to E·Met	K_4	0.043
P_i binding to E·AdoMet·PP_i	K_7	14[b]
PP_i binding to E·AdoMet·P_i	K_8	ND[c]
PP_i binding to E·AdoMet	K_9	0.053
P_i binding to E·AdoMet	K_{10}	ND[c]
AdoMet binding to E	K_{11}	0.021
PPP_i binding to E·AdoMet	K_{12}	0.0025

[a] Binding was determined by quenching of protein fluorescence except in the case of P_i. [b] Concentration of P_i yielding half-maximal formation E·AdoMet·PPP_i from E·AdoMet·PP_i·P_i. [c] ND, not determined since these steps do appear on the primary kinetic pathway.

Determination of Equilibrium Binding Constants

Binary Enzyme−Substrate Complexes. The equilibrium constant for binding of most substrates and products to the enzyme could be measured from decreases in intrinsic enzyme fluorescence upon binding (excited at 295 nm, monitored at 333−345 nm); see Table 1. The binding of ATP to free enzyme is fairly weak (K_d = 1.4 mM); this K_d value corresponds closely to the K_m of 1.3 mM for ATP in the hydrolytic reaction that yields ADP and P_i at a rate of ∼0.002 turnovers/s (*15*); at the low concentrations of enzyme used, substrate depletion was negligible during the binding experiments. Methionine binding also caused quenching of the protein florescence, allowing measurement of a dissociation constant of 0.58 mM. Since the in vivo concentrations of ATP and methionine are ca. 3 and 0.1 mM, respectively (*38*, *43*), under physiological conditions ATP will presumably bind before methionine in the predominant kinetic path. Interestingly, steady-state kinetic studies of AdoMet synthetases from other organisms have indicated an ordered mechanism with ATP binding first (*44*, *45*).

Dissociation Constants for Ternary Enzyme−Substrate Complexes. The equilibrium constant for methionine binding to E·ATP was obtained by measuring the fluorescence quenching of the E·ATP complex upon titration with methionine (Figure 1A). Although enzyme turnover occurs under these conditions, the amount of substrate depletion is minimal due to the low concentration of enzyme (0.04 μM). The 25 μM dissociation constant thus obtained represents an upper limit for the affinity of methionine for the E·ATP complex due to the presence of the small amount of products. Unfortunately, no ATP analogue has yet been found that binds to the enzyme but is neither a substrate for AdoMet synthesis or rapid hydrolysis, preventing evaluation of methionine binding to a nonreactive ternary complex.

In similar experiments, measurements of the binding of ATP to the E·Met complex yielded an apparent dissociation constant of 43 μM. The ATP dissociation constant decreased to 110 μM when the inhibitory methionine analogue L-*cis*-2-amino-4-methoxybutanoic acid was used instead of methionine [employed at 0.35 mM, 4-fold higher than its K_i value (*31*)], substantiating the increase of affinity of the enzyme for ATP when the methionine site is occupied.

Intermediate and Product Binding. The dissociation constant for the binding of AdoMet to the free enzyme was determined to be 21 μM from protein fluorescence quenching experiments. The equilibrium constant of 53 μM for the binding of PP_i to E·AdoMet was determined by measurement of the decrease in enzyme fluorescence upon PP_i binding in the presence of saturating AdoMet. Binding of P_i to the free enzyme, or enzyme complexes, could not be measured in this fashion due to the lack of a fluorescence change. The dissociation constant for P_i from the E·AdoMet·PP_i·P_i complex was estimated as 14 mM from the concentration dependence for formation of enzyme-bound PPP_i from PP_i and P_i. The apparent dissociation constant is in accord with the values for noncompetitive inhibition of the AdoMet synthetase reaction by P_i (8−25 mM) (*15*). Since the enzyme's affinity for P_i is more than 100-fold lower than for either AdoMet or PP_i, the product release route in which P_i is the first product to dissociate was emphasized in further experiments (the top route in Scheme 1).

A dissociation constant of 2.5 μM for the binding of PPP_i to the E·AdoMet complex was obtained from fluorescence quenching; in this case there is the caveat that PPP_i is hydrolyzed during the titration. Nevertheless, the slow consumption of PPP_i at the low enzyme concentration and the higher affinity of the enzyme for PPP_i compared to PP_i and P_i make this dissociation constant a reasonable approximation to the true value, and it is comparable to the 8 μM K_i value determined for competitive inhibition with respect to ATP (*15*).

Determination of the Kinetic Competence of Binary Enzyme−Substrate Complexes

Previous steady-state kinetic experiments indicated that ATP and methionine bind randomly (*15*). This conclusion was supported by kinetic isotope effect studies which showed that both ATP and methionine can dissociate from the E·ATP·Met complex (*17*). The kinetic competence of the binary enzyme−substrate complexes was examined by substrate trapping (pulse−chase) experiments (*36*, *37*).

The ATP trapping experiment involved premixing [8-^{14}C]-ATP with AdoMet synthetase, followed by mixing with a solution of methionine and excess unlabeled ATP. If the E·[8-^{14}C]ATP complex initially present is kinetically competent, the experiment can result in the formation of radiolabeled product. The amount of radiolabeled product formed is a function of the partitioning of the E·[8-^{14}C]ATP complex between reaction with methionine and dissociation. The amount of trapping is therefore dependent on the methionine concentration, and the concentration that yields half-maximal trapping can be used to estimate the dissociation rate k_{off} of ATP from the E·ATP complex (*37*).

A time course of trapping of ATP was determined by mixing a solution of AdoMet synthetase (0.1 mM active sites) and [8-^{14}C]ATP (0.6 mM) with an equal volume of a solution containing 44 mM ATP and 14 mM methionine. At several times after mixing the reactions were quenched and analyzed as described in Materials and Methods. The results shown in Figure 2A show a rapid accumulation of radiolabeled product which then levels off to the rate found in control experiments in which the [8-^{14}C]ATP was initially in the chase rather than with the enzyme. The amount of trapping corresponds to 56% of the E·ATP that was calculated to be initially bound in the pulse. This experiment shows that

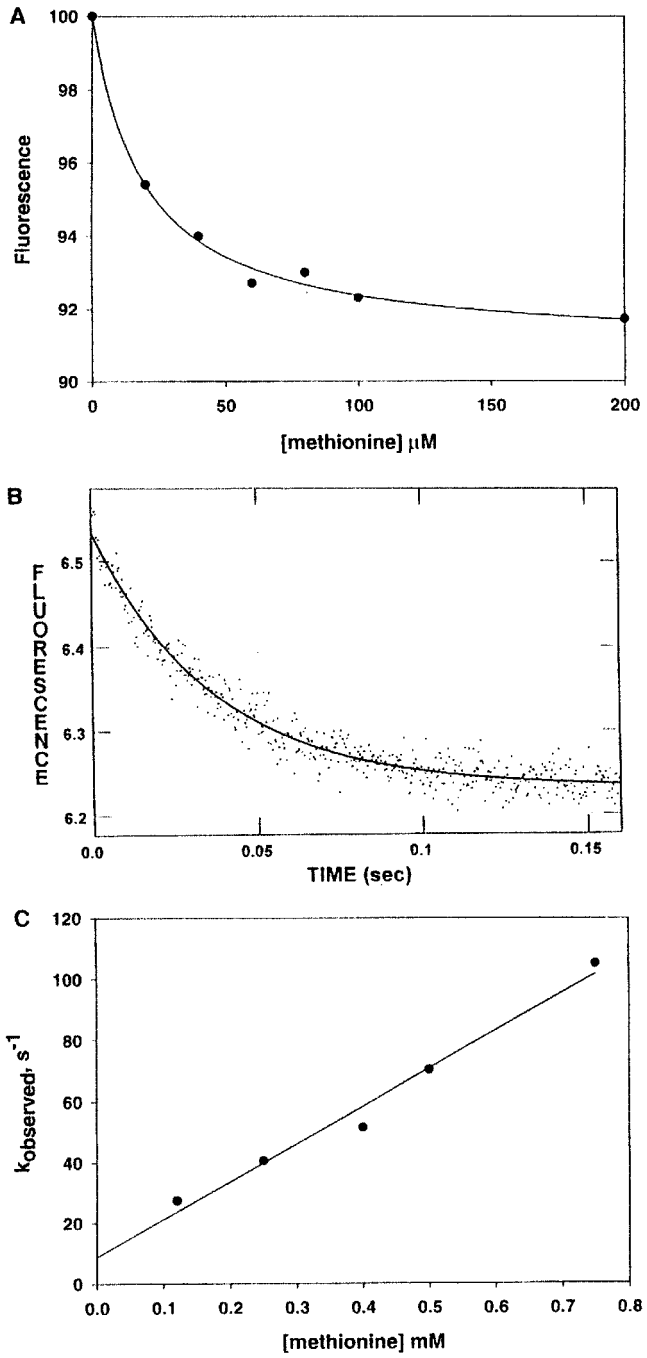

FIGURE 1: Part A shows binding of methionine to the binary E·ATP complex as measured by quenching of protein fluorescence. Solutions contained 0.04 μM AdoMet synthetase, 12 mM ATP, and various amounts of methionine. The line is a fit to an equilibrium constant of 25 μM. Part B shows the time course of a typical binding experiment monitoring the rate of binding of methionine to the E·ATP complex as measured by stopped-flow fluorescence. The solution contained 2.5 μM enzyme, 5 mM ATP, and 125 μM methionine (after mixing). The solid line is a single-exponential fit to the observed data with a rate constant of 26 s^{-1}. Part C shows the plot of observed rate vs methionine concentration. The slope of the line gives the binding rate of 0.16 μM^{-1} s^{-1}, and the vertical intercept gives the dissociation rate of 10 s^{-1}.

AdoMet synthesis can proceed by ATP binding before methionine and that the rate of ATP dissociation from the ternary E·ATP·Met complex is comparable to the rate of product formation. This observation is consistent with the kinetic isotope effect studies which showed a significant

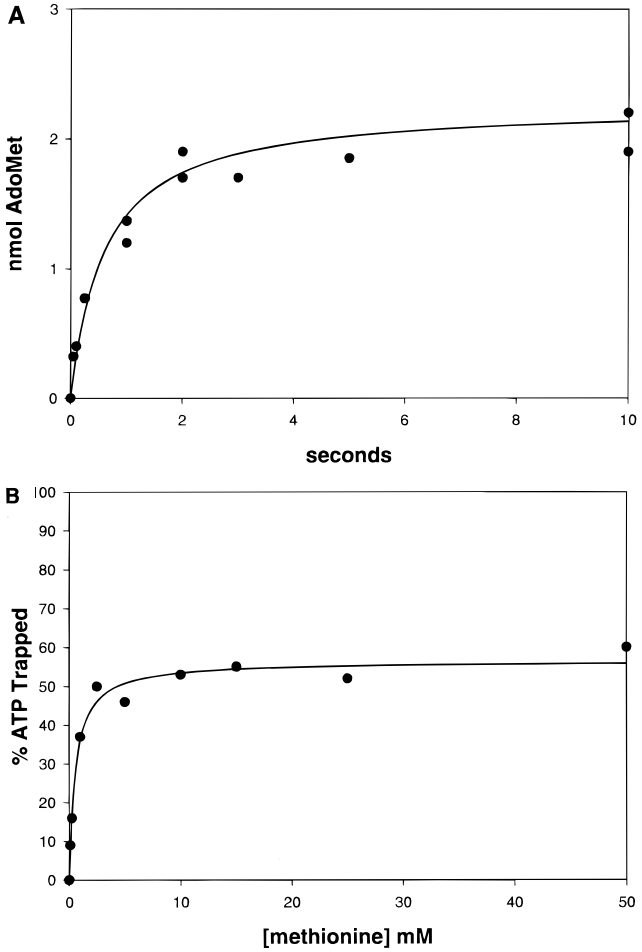

FIGURE 2: Determination of the kinetic competence of binary enzyme−substrate complexes by substrate trapping (pulse−chase) experiments. Part A shows the time course for trapping of ATP. A solution containing 0.6 mM [8-^{14}C]ATP and 0.1 mM enzyme was mixed with an equal volume of 44 mM ATP, 44 mM $MgCl_2$, and 14 mM methionine. After the indicated incubation times, reactions were terminated and AdoMet was analyzed as described in Materials and Methods. Part B shows the dependence of ATP trapping on methionine concentration after a 10 s incubation.

commitment to catalysis for ATP at high methionine concentrations (*17*).

To obtain an estimate for the dissociation rate of ATP from the E·ATP complex (k_{-1} in Scheme 1), the amount of methionine required in the chase for half-maximal trapping of ATP was determined. A solution of 0.1 mM [8-^{14}C]ATP and 0.2 mM enzyme was mixed with a solution containing 28 mM ATP and various amounts of methionine (0.2−100 mM). The amount of ATP trapped was measured after 10 s. The amount of methionine required for half-maximal trapping ($K_{t,Met}$) was 0.5 mM (Figure 2B). Limits for the ATP dissociation rate from the binary enzyme·ATP complex, k_{-1}, can be calculated using the equation

$$k_{cat}\left(\frac{K_{t,Met}}{K_{m,Met}}\right) < k_{-1} < \frac{K_{t,Met}}{K_{m,Met}} k_{cat} \frac{[E{\cdot}ATP^*]}{P^*\infty} \qquad (3)$$

where $K_{m,Met}$ is the Michaelis constant for methionine (0.08 mM), $P^*\infty/[E{\cdot}ATP^*]_0$ is the fraction of the initially bound ATP that is trapped at saturating methionine (0.56), and k_{cat} equals 1.5 s^{-1} (*37*). These values indicate that k_{-1} is within the range of 9−16 s^{-1}. Furthermore, the dissociation rate of

ATP from the ternary E·ATP·Met complex must be as large as

$$k_{-4} \geq k_{cat}\left(\frac{[E\cdot ATP^*]}{P^*_\infty} - 1\right) \quad (4)$$

which is 1.0 s^{-1}; the value of k_{-4} estimated from the kinetic isotope experiments was 7 s^{-1} (*17*).

An analogous pulse−chase experiment was performed in order to determine if a binary E·Met complex could be trapped. A solution of [*methyl*-^{14}C]methionine (0.6 mM) and 100 μM AdoMet synthetase was mixed with an equal volume of a solution containing 44 mM methionine and 14 mM ATP. The amount of trapped methionine was small and corresponds to ca. 9% of the E·Met complex initially present. The low amount of trapping is consistent with the kinetic isotope effect studies that showed no significant commitment to catalysis for methionine, suggesting that methionine dissociation from the ternary E·ATP·Met complex is rapid with respect to the forward reaction (*17*).

The dependence of methionine trapping on ATP concentration was not investigated in detail due to the small amount of the E·Met complex trapped; however, approximately half as much methionine was trapped at 1 mM ATP as at 14 mM ATP, allowing an estimate of a lower limit on the dissociation rate of methionine from the ternary complex (k_{-3}) of 15 s^{-1}. If the $K_{t,ATP}$ is 1 mM, in combination with the ATP K_m of 0.11 mM, a dissociation rate of the binary E·Met complex is calculated to be between 14 and 150 s^{-1}.

Stopped-Flow Fluorescence Measurements of Binding Rate Constants for Substrates

For ligands that produced changes in intrinsic enzyme fluorescence, their binding rates were measured by following the kinetics of the fluorescence change using stopped-flow techniques. Since the previous studies suggested that the predominant kinetic pathway had ATP binding before methionine, this pathway was emphasized.

Rate of ATP Binding. The observed rate constant for ATP binding to the enzyme showed a linear concentration dependence in the range of 0.12−1.5 mM. Analysis as described in Materials and Methods yielded a binding rate constant, k_1, of 0.0086 μM^{-1} s^{-1} and an estimate of the dissociation rate of 8 s^{-1}. From these values a dissociation constant of 0.9 mM is calculated, in good agreement with the measured value of 1.3 mM. The binding rate constant is also reasonably consistent with the k_{cat}/K_m value for ATP in the AdoMet synthetase reaction of 0.013 μM^{-1} s^{-1}.

Rate of Methionine Binding to E·ATP. The rate of methionine binding to the E·ATP complex was measured similarly. Figure 1B shows a typical stopped-flow trace. The observed rate constant for binding was linearly dependent on methionine concentration in the range of 0.1−0.75 mM. The slope of the plot of the observed rate constant vs substrate concentration (Figure 1C) yielded the methionine association rate constant, k_3, of 0.16 μM^{-1} s^{-1}, and the intercept provided an estimate of the dissociation rate constant, k_{-3}, of 10 s^{-1}. These values allow calculation of the dissociation constant for methionine binding to E·ATP of 62 μM, in reasonable agreement with the measured value of 25 μM. The value of the rate constant for binding, k_3, is 8-fold larger than the k_{cat}/K_m value of 0.02 μM^{-1} s^{-1}. The value of k_{-3} estimated from the stopped-flow results is less than the value estimated from the pulse−chase experiment. These observations suggest that this binding process may involve an unimolecular event that does not affect the protein fluorescence.

Rate of AdoMet Binding. The rate constant for AdoMet binding was determined analogously using a concentration range from 5 to 50 μM. The plot of rate vs concentration was linear and gave a second-order binding rate constant, k_{-11}, of 0.25 μM^{-1} s^{-1}, and the intercept provided a dissociation rate constant, k_{11}, of 3.4 s^{-1}. From these values a dissociation constant of 13 μM is calculated, comparable to the measured value of 21 μM. When the rate of AdoMet binding was measured in the presence of 5 mM PP_i, again the observed rate constant showed a linear dependence on AdoMet concentration; association and dissociation rate constants of 0.028 μM^{-1} s^{-1} and 0.27 s^{-1} were obtained. This provides an estimate of the dissociation constant of 10 μM, in reasonable agreement with the measured value of 20 μM. Interestingly, both the binding and dissociation rates of AdoMet decrease in the presence of PP_i. Since the dissociation rate is 5-fold less than k_{cat} for AdoMet synthesis, this result supports the deduction from steady-state experiments that during turnover AdoMet dissociation follows PP_i release (*15*).

Rate of PP_i Binding to E·AdoMet. The rate constant for PP_i binding was also determined by stopped-flow fluorescence measurements, using PP_i concentrations from 25 to 250 μM in the presence of 1 mM AdoMet. The plot of rate vs concentration was linear and gave a second-order association rate constant (k_{-9}) of 0.072 μM^{-1} s^{-1} and an estimate of the dissociation rate (k_{-9}) of $\leq$5 s^{-1}. From the measured dissociation constant of PP_i from the E·AdoMet·PP_i complex of 53 μM and the measured binding rate, a dissociation rate constant of 4 s^{-1} would be expected, which would be consistent with the turnover rate of the enzyme.

Rate of P_i Binding to E·AdoMet·PP_i. The rate constant for P_i association was determined by measuring the rate of $^{32}PPP_i$ formation at low P_i concentration. Thus 50 μM enzyme was incubated with 1 mM AdoMet, 4 mM PP_i, and 4 μM $^{32}P_i$ (final concentrations). Under these conditions the reaction rate is determined by the rate of P_i binding. The rate constant for P_i binding (k_7) of 0.045 μM^{-1} s^{-1} was thus determined. From this value, and the dissociation constant of 14 mM, a dissociation rate (k_8) of 310 s^{-1} is calculated. This dissociation rate is nearly 100-fold larger than any other measured product dissociation rate, indicating that during turnover P_i is the first product to dissociate. In light of this finding, the alternate pathway in which PP_i is the first product released was not further studied.

Rate of PPP_i Binding to E·AdoMet. To fully characterize the PPP_i hydrolysis reaction, the kinetic constants associated with PPP_i binding were measured. The rate of PPP_i binding to the E·AdoMet complex was determined by mixing a solution of enzyme and AdoMet with concentrations of PPP_i from 0.025 to 5 mM. The observed rates for PPP_i concentrations greater than 0.5 mM were not proportional to PPP_i concentration and maximized at a rate of ~33 s^{-1} (Figure 3). This observation indicates a two-step binding process where the initial complex formation described by K_{12} is followed by an isomerization described by $K_{12,iso}$ (with forward and reverse rate constants $k_{12,iso}$ and $k_{-12,iso}$; Scheme

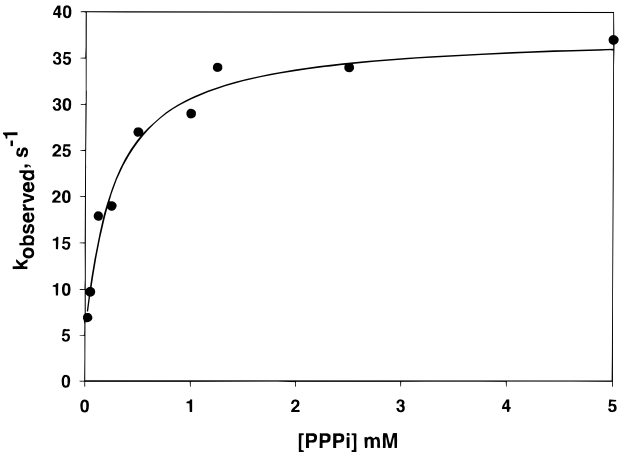

FIGURE 3: Determination of the rate of binding of PPP_i to the E·AdoMet complex. The binding rate was monitored by changes in protein fluorescence in a stopped-flow instrument. Final concentrations were 2.5 μM AdoMet synthetase, 0.4 mM AdoMet, and 0.025−5 mM PPP_i. The line is a fit of the observed rate constants to eq 5. The analysis yields an equilibrium constant for the initial complex of 0.27 mM and the forward and reverse rate constants for the conformational change of 33 s^{-1} and 4 s^{-1}. This analysis assumes rapid equilibrium in the initial encounter complex (*27*).

2). The pseudo-first-order rate constants at various PPP_i concentrations were fit to the equation (*27*):

$$k_{obsd} = k_{-12,iso}[PPP_i]/([PPP_i] + K_{12}) + k_{12,iso} \quad (5)$$

This analysis provides an estimate of the equilibrium constant for the initial binding of PPP_i (K_{12}) of 0.27 mM, the rate constant of the subsequent forward ($k_{-12,iso}$) process of 33 s^{-1}, and the rate constant for reversal of the isomerization step, $k_{12,iso}$, of 4 s^{-1}. A lower limit for the binding rate constant (k_{-12}) is $k_{-12,iso}/K_{12} = 0.12$ μM^{-1} s^{-1}, which compares well to the k_{cat}/K_m value of 0.092 μM^{-1} s^{-1}. K_{12} and k_{-12} allow calculation of the PPP_i dissociation rate k_{12} of 30 s^{-1}. The 4 s^{-1} value of the slow step in dissociation is inconsistent with the failure of 98% of the PPP_i to escape the active site during the AdoMet synthetase reaction, which indicates a dissociation rate of less than 2% the hydrolytic rate or <0.06 s^{-1} (*15*). The net dissociation constant estimated as $K_{12}k_{12,iso}/(k_{12,iso} + k_{-12,iso})$ is 29 μM, which is also in poor agreement with the value of 2.5 μM observed in the binding experiments. Thus another process may occur during binding but does not cause changes in protein fluorescence. Since the binding of PPP_i is not part of the overall AdoMet synthetase reaction, this possibility was not further investigated. The data indicate that the conformational change which occurs after PPP_i binding has a rate ca. 10-fold greater than the turnover rate of the PPP_i hydrolytic reaction. This was the only ligand binding process that showed the clear presence of a kinetically significant step following the initial enzyme−ligand interaction.

Rate of Reversal of AdoMet Synthesis. The rate of [^{32}P]-ATP formation was obtained by monitoring reactions at high concentrations of enzyme with $^{32}PP_i$, AdoMet, and P_i for up to 5 h. The observed rate was 1.5×10^{-4} s^{-1}. Since only part of the enzyme would be in the reactive E·AdoMet·PPP_i complex due to its equilibrium with the E·AdoMet·PP_i·P_i complex (see below), the observed rate of ATP formation provides a lower limit on the rate constant. This observed value is comparable to the upper limit of 10^{-4} s^{-1} estimated

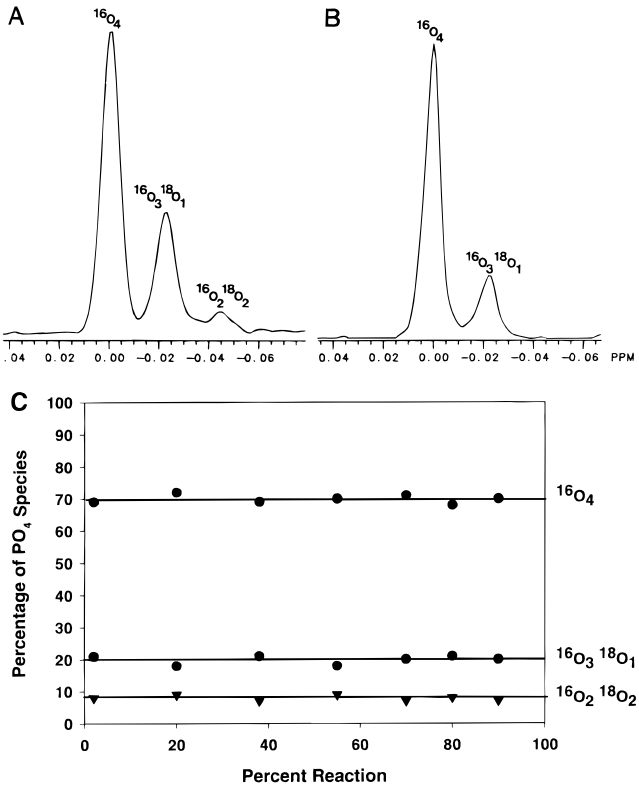

FIGURE 4: ^{18}O incorporation from $H_2{}^{18}O$ into P_i formed in reactions catalyzed by AdoMet synthetase. Solutions contained 5.5 mM ATP and 5.5 mM methionine, or 5.5 mM PPP_i, in 22% $H_2{}^{18}O$. Parts A and B compare ^{31}P NMR spectra obtained for the P_i formed in the two reactions. Part C shows the percentage of each P_i species formed as a function of percent conversion of ATP and methionine to products in the AdoMet synthetase reaction. Solutions contained 50 mM Hepes−KOH, 50 mM KCl, 10 mM $MgCl_2$, and 10% D_2O.

for the reversal of the reaction of AMPPNP and methionine using isotope dilution methods (*15*).

Solvent Oxygen Incorporation into P_i Formed during Turnover

To investigate whether a kinetically significant process occurred after PPP_i hydrolysis, the incorporation of ^{18}O from $H_2{}^{18}O$ into P_i was monitored by ^{31}P NMR. As illustrated in Figure 4, during the AdoMet synthetase reaction the incorporation of ^{18}O exceeded the single equivalent required for hydrolysis, as is most obviously evident as a signal from $P^{16}O_2{}^{18}O_2$. The same amount of excess ^{18}O was incorporated into the P_i formed during the AdoMet synthetase reaction and during PPP_i hydrolysis in the presence of AdoMet. These results indicate the reversal of the hydrolytic reaction before product release. In contrast, Figure 4B illustrates that the 20-fold slower PPP_i hydrolytic reaction in the absence of AdoMet yielded P_i with the same ^{18}O content as the $H_2{}^{18}O$, indicating rapid product release compared to reversal of the hydrolytic reaction. Figure 4C shows that the same distribution of PO_4 species was observed throughout the course of the AdoMet synthetase reaction, demonstrating that the excess O^{18} incorporation did not result from reversal of the reaction from free products. Quantitative analysis of the relative amounts of the isotopomers as described by Hackney (*46*) indicates that the E·AdoMet·PP_i·P_i complex partitions equally between dissociation and resynthesis of PPP_i (a partition coefficient of 0.50 ± 0.05). In light of the rapid

Table 2: Kinetic Constants for Steps in the AdoMet Synthetase Reaction (As Labeled in Scheme 1)

interaction	parameter	value[a] measured	value[a] calculated[c]	method[b]
E + ATP → E·ATP	k_1	0.0085		SF-F
E·ATP → E + ATP	k_{-1}	8, 9−16		SF-F, IT
E + Met → E·Met	k_2		0.025−0.53	
E·Met → E + Met	k_{-2}	14−150		IT
E·ATP + Met → E·Met·ATP	k_3	0.16		SF-F
E·Met·ATP → E·ATP + Met	k_{-3}	10, ≥15		SF-F, IT
E·Met + ATP → E·ATP·Met	k_4		0.016	
E·ATP·Met → E·Met + ATP	k_{-4}	≥1, 7		IT, KIE
E·ATP·Met → E·AdoMet·PPP_i	k_5	1.5		overall k_{cat}
E·AdoMet·PPP_i → E·ATP·Met	k_{-5}	1.5×10^{-4}		reverse reaction
E·AdoMet·PPP_i → E·Ado·PP_i·P_i	k_6	3.1		PPP_iase k_{cat}
E·AdoMet·PP_i·P_i → E·AdoMet·PPP_i	k_{-6}	ND		
E·AdoMet·PP_i·P_i → E·AdoMet·PP_i + P_i	k_7		310	
E·AdoMet·PP_i + P_i → E·AdoMet·PP_i·P_i	k_{-7}	0.045		ST
E·AdoMet·P_i·PP_i → E·AdoMet·P_i + PP_i	k_8	ND		
E·AdoMet·P_i + PP_i → E·AdoMet·PP_i·P_i	k_{-8}	ND		
E·AdoMet·PP_i → E·AdoMet + PP_i	k_9		4	
E·AdoMet + PP_i →E·AdoMet·PP_i	k_{-9}	0.072		SF-F
E·AdoMet·P_i → E·P_i + AdoMet	k_{10}	ND		
E·P_i + AdoMet → E·AdoMet·P_i	k_{-10}	ND		
E·AdoMet → E + AdoMet	k_{11}	3.4		SF-F
E + AdoMet → E·AdoMet	k_{-11}	0.25		SF-F
E·AdoMet·PPP_i → E·AdoMet + PPP_i	k_{12}	30		SF-F
E·AdoMet + PPP_i → E·AdoMet·PPP_i[d]	k_{-12}	0.12		SF-F

[a] Bimolecular rate constants are in units of μM^{-1} s^{-1} and unimolecular rate constants in s^{-1}. [b] Abbreviations: IT, isotope trapping; QF, chemical quench flow; SF-F, stopped-flow fluorescence; ST, single turnover at subsaturating substrate; KIE, kinetic isotope effect (*17*); ND, not determined. [c] Calculated from the measured association rate constant and the equilibrium constant listed in Table 1. [d] This process is biphasic. A unimolecular process with an observed rate of 33 s^{-1} follows the initial binding rate (see Results).

dissociation rate of P_i, these data indicate that an additional complex, *E·AdoMet·PP_i·P_i*, must form by isomerization of the E·AdoMet·PP_i·P_i complex before product release in order to allow time for the resynthesis of PPP_i (Scheme 2).

Time Courses for Single Turnover and Computer Modeling

The time courses for a single turnover of PPP_i hydrolysis and formation, as well as for the AdoMet synthetase reaction, were determined using quench-flow techniques (Figure 5). The time course for the AdoMet synthetase reaction showed the formation and decay of the PPP_i intermediate (Figure 5A). Data analysis for these reactions used simulation with the KINSIM and FITSIM programs (*40*−*42*). The simulation strategy exploited the observation that the PPP_i hydrolytic reaction is kinetically uncoupled from the synthetase reaction due to the slow reversal of the AdoMet synthesis step. Thus the PPP_i hydrolysis segment was initially analyzed in detail in both reaction directions; those kinetic constants were then carried over to the overall AdoMet synthetase reaction. The curves shown in Figures 5 were obtained using the rate constants listed in Table 3. It was not possible to obtain satisfactory fits to the time courses for the PPP_i hydrolytic and synthesis reactions without inclusion of the isomerization of the E·AdoMet·PP_i·P_i complex. These simulations provided values for k_{-6}, $k_{6,iso}$, and $k_{-6,iso}$ for Scheme 2 and thus completed the determination of the rate constants for a minimal kinetic scheme. The simulations showed that the values of k_{+6} and $k_{+6,iso}$ are tightly coupled in providing a good fit to the data, and changes in values on the order of 50% could provide an improved fit of an individual data set at the detriment to the fits to the other data. In this scheme the reverse of the isomerization step $k_{-6,iso}$ is the rate-limiting step in the formation of PPP_i from PP_i and P_i. The apparent equilibrium constant for the PPP_i hydrolytic reaction is determined by the product of K_6 and $K_{6,iso}$, yielding a value of 190 although the equilibrium constant for the chemical step itself is 0.6.

DISCUSSION

The free energy profile for the AdoMet synthetase reaction is illustrated in Figure 6. Published bacterial concentrations of ATP, methionine, AdoMet, PP_i, and P_i were used to set the standard state (*38*, *43*, *47*, *48*). The free energy profile shows that the members of the group of substrate-containing species (E + ATP + Met), (E·ATP + Met), and (E·ATP·Met) are comparable in energy, facilitating flux toward the central complex. Similarly, the group of product-containing species (E + AdoMet + PP_i + P_i), (E·AdoMet + PP_i + P_i), (E·AdoMet·PP_i + P_i), and (*E·AdoMet·PP_i·P_i*) are similar in energy, which will facilitate product release. Both of these groups of complexes, which are in direct communication with the solution environment, are offset in energy from the internal E·AdoMet·PPP_i and E·AdoMet·PP_i·P_i complexes by 3−5 kcal/mol, whereas the internal complexes are themselves better energetically balanced, expediting interconversion. The overall favorable free energy of the reaction is manifest in the combination of the AdoMet-forming reaction and the isomerization of the E·AdoMet·PP_i·P_i complex, both of which have large free energy changes favoring product formation. The highly exergonic AdoMet-forming step puts the enzyme in a deep thermodynamic well. Thus hydrolysis

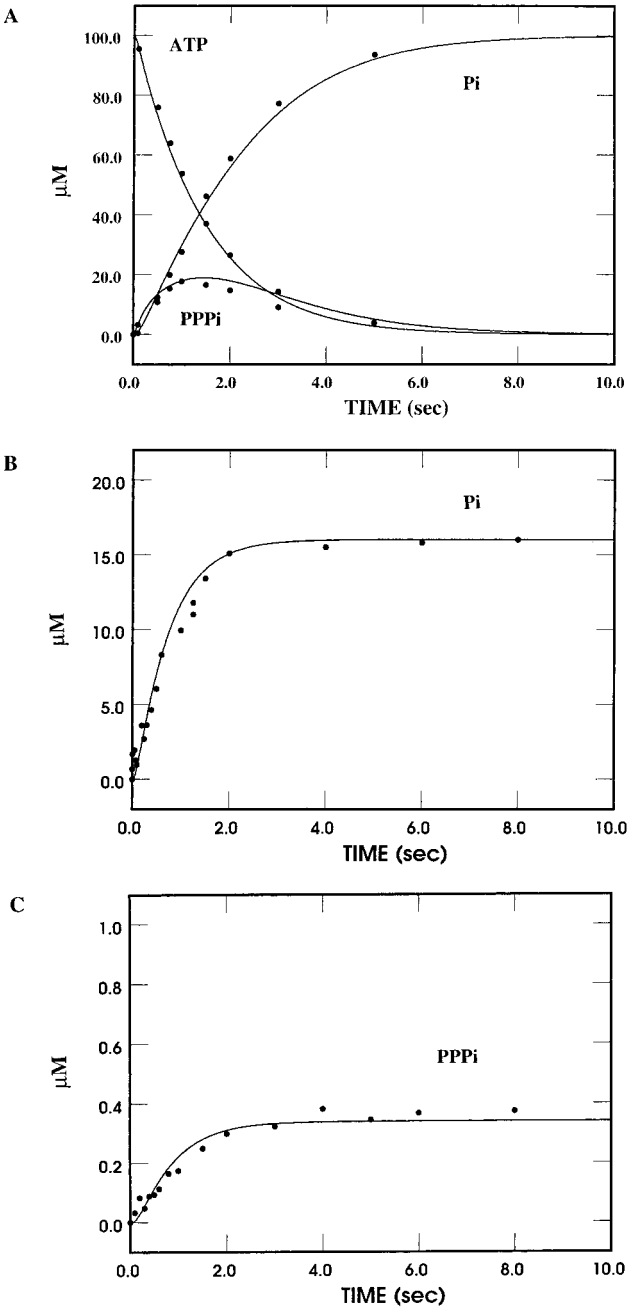

FIGURE 5: Time courses for single turnover experiments. Part A shows the time course for a single turnover of the AdoMet synthetase reaction. Solutions contained 130 μM AdoMet synthetase, 100 μM ATP, and 10 mM methionine. Lines were obtained by fitting using KINSIM and FITSIM with the kinetic constants listed in Table 3. Conditions for product analysis are described in Materials and Methods. Part B shows the time course for a single turnover of PPP_i hydrolysis. Solutions contained 60 μM AdoMet synthetase, 1 mM AdoMet, and 16 μM $^{32}PPP_i$. Part C shows the time course for a single turnover of PPP_i synthesis when the enzyme−AdoMet complex was mixed with $^{32}PP_i$ and P_i. Solutions contained 60 μM AdoMet synthetase, 1 mM AdoMet, 20 μM $^{32}PP_i$, and 30 mM P_i.

of the PPP_i intermediate is needed to liberate the enzyme from this trap and allow efficient turnover. This is consistent with previous findings that the enzyme-bound equilibrium formed from reaction of methionine with nonhydrolyzable ATP analogues β,γ-imido-ATP (AMPPNP) and $\alpha,\beta:\beta,\gamma$-diimido-ATP (AMPNPNP) greatly favored product formation (*15*, *18*). However, our recent discovery that both diimidotriphosphate and imidodiphosphate have unusually high affinity for the enzyme (*21*) rendered tenuous the extrapolation from the analogues to ATP itself. The hydrolytic reaction has a more balanced internal equilibrium constant of 0.6 for the chemical step, but the reaction is pulled by the favorable equilibrium constant of the subsequent isomerization. When the isomerized enzyme reverts to the original form remains elusive. The near unity equilibrium constant for the chemical step of PPP_i hydrolysis is reminiscent of the internal equilibrium constants near unity found for many other enzymes, particularly those involved in phosphoryl transfer (*49*, *50*). For comparison, the enzyme-bound equilibrium constant for the hydrolysis of PP_i by inorganic pyrophosphatase has been reported in the range of 0.11−0.25 (*51*).

The crystal structures of apo and liganded AdoMet synthetase have implied that movement of a surface loop is important in enzyme function (*25*). The loop is closed but is in slightly different conformations in the two crystallographically independent subunits present in the apo-enzyme structure (*25*); both of these conformations would hinder access of substrates to their binding sites. In the crystal structures with bound ligands, the loop is disordered,

Table 3: Kinetic Constants Used in Simulations of the Single Turnover Time Courses (Scheme 2 and Figure 5)[a]

step	k_+	k_-	step	k_+	k_-
1	0.0086	8	6 iso	12	0.04
2	0.25	150	7	310	0.045
3	0.16	5	9	4	0.065
4	0.16	15	11	3.4	0.25
5	1.2	0.00015[b]	12	0.44	0.11
6	9	14	12 iso	4	33

[a] Bimolecular rate constants are in units of μM^{-1} s^{-1} and unimolecular rate constants in s^{-1}. [b] The simulations were not sensitive to this value.

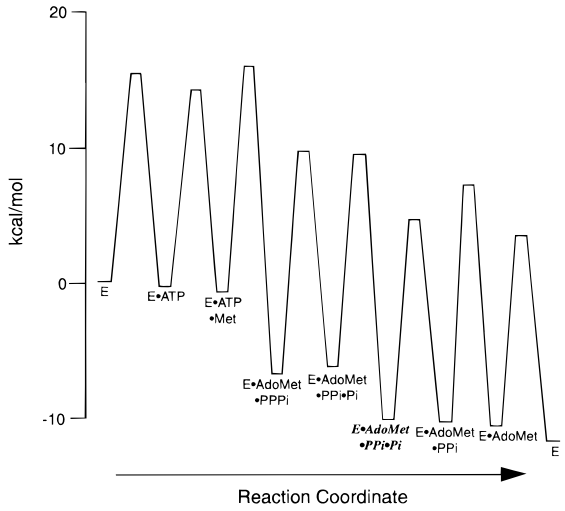

FIGURE 6: Free energy profile for the AdoMet synthetase reaction. The profile was constructed using the values in Table 3 and the intracellular concentrations of ATP (2.6 mM), methionine (0.1 mM), AdoMet (0.08 mM), PP_i (0.5 mM), and P_i (9 mM) (*38*, *43*, *47*, *48*). The isomerized E·AdoMet·PP_i·P_i complex is shown in italic. ΔG values for equilibria were calculated from $\Delta G = -RT \ln K$, where R is the gas constant. Activation energies were calculated from the equation $\Delta G^{\ddagger} = -RT \ln[kh/(k_bT)]$, where h is Planck's constant and k_b is Boltzmann's constant. Second-order rate constants were converted to effective first-order physiological rate constants using the in vivo ligand concentrations.

suggesting dynamic properties. It is noteworthy that crystal structures with methionine or AdoMet have not been obtained; thus it is possible that the loop stabilizes in conjunction with formation of complexes containing these ligands. The observed protein fluorescence changes upon substrate−product binding also suggest that conformational changes occur, since the crystal structures show that the closest of the four tryptophan residues is ∼15 Å from the active site. However, while all of the tryptophans are at least partially exposed on the protein surface, none is in the loop region (*23*). The present results show that all of the substrate and product binding rates are on the order of 10^4-10^5 M^{-1} s^{-1}, $>10^3$-fold less than the diffusion limit, and are of the same magnitude as k_{cat}/K_m values seen in steady-state kinetic studies; these low substrate association rates suggest that binding is a multistep process (*27*). The similar values of the binding rate constants for structurally diverse ligands suggest that the rate of loop movement has pronounced effects on the association rates and that the loop movement occurs at similar rates in the presence and absence of ligands. However, the only kinetic data that directly reflect an isomerization coordinated with ligand binding are those for PPP_i binding to the enzyme−AdoMet complex where a first-order process with a rate of 33 s^{-1} occurs after binding. Even though this process is not on the pathway for the overall reaction, it does reflect a dynamic process of which the enzyme is capable. The structural relationship, if any, between the isomerization following PPP_i binding and that of the E·AdoMet·PP_i·P_i complex is as yet unclear. Since there are no tryptophan residues in the loop region, it is not surprising that a fluorescence change associated with the loop movement is not observed. However, one might have expected to see deviations from linearity in the concentration dependence of observed binding rates for other ligands; the failure to see limiting unimolecular rates indicates that in most cases any process gating binding is faster than the largest rate observed in our experiments, greater than 120 s^{-1} in the case of methionine binding.

Although the loop residues appear not to directly interact with the substrates, mutations in the loop can have dramatic effects on enzyme activity. The k_{cat} is reduced by 1000-fold (with less than 2-fold changes in K_m values) when the center of the loop sequence (^{107}DRADPLEQ) is replaced by the sequence of the rat liver enzyme (HLDRNEEDV) (*52*); the rat liver enzyme itself has a ca. 100-fold lower k_{cat} than for the *E. coli* enzyme although the active site residues are all conserved (*53*). Interestingly, in the rat liver enzyme nitric oxide modification of cysteine-121 at the N-terminal edge of the loop has been correlated with impairment of catalytic activity (*53*). The present results lead to the speculation that the isomerization of the E·AdoMet·PP_i·P_i complex that occurs prior to product release is reorientation of the loop to allow product dissociation. Further comparisons of the kinetic properties of mutant enzymes with variations in the loop sequence will be informative in elucidating the dynamics of loop motion and the reasons underlying slow substrate binding.

ACKNOWLEDGMENT

We thank Dr. D. Chapman for use of the fluorescence spectrofluorometer. Helpful discussions with Dr. R. S. Reczkowski are acknowledged.

REFERENCES

1. Cantoni, G. L. (1975) *Annu. Rev. Biochem. 44*, 435−451.
2. Mudd, S. H. (1973) in *The Enzymes* (Boyer, P. D., Ed.) Vol. 8, pp 121−154, Academic Press, New York.
3. Tabor, C. W., and Tabor, H. (1984) *Adv. Enzymol. 56*, 251−282.
4. Mato, J. M., Alvarez, L., Ortiz, P., and Pajares, M. A. (1997) *Pharmacol. Ther. 73*, 265−280.
5. Salvatore, F., Borek, E., Zappia, V., Williams-Ashman, H. G., and Schlenk, F., Eds. (1977) *The Biochemistry of Adenosylmethionine*, Columbia University Press, New York.
6. Usdin, E., Borchardt, R. T., and Creveling, C. R. (1982) *Biochemistry of S-adenosylmethionine and related compounds*, Macmillan Press, London.
7. Chiang, P. K., Gordon, R. D., Tal, J., Zeng, G. C., Doctor, B. P., Pardhasaradhi, K., and McCann, P. P. (1996) *FASEB J. 10*, 471−480.
8. Aletta, J. M., Cimato, T. R., and Ettinger, M. J. (1998) *Trends Biol. Sci. 23*, 89−91.
9. Pegg, A. E. (1988) *Cancer Res. 48*, 759−774.
10. Tabor, C. W., and Tabor, H. (1984) *Annu. Rev. Biochem. 53*, 749−790.
11. Frey, P. A., Ballinger, M. D., and Reed, G. H. (1998) *Biochem. Soc. Trans. 26*, 304−310.
12. Hastings, J. W., and Greenberg, E. P. (1999) *J. Bacteriol. 181*, 2667−2668.
13. Yang, S. F., and Hoffman, N. E. (1984) *Annu. Rev. Plant Physiol. 35*, 155−189.
14. Mudd, S. H. (1963) *J. Biol. Chem. 238*, 2156−2163.
15. Markham, G. D., Hafner, E. W., Tabor, C. W., and Tabor, H. (1980) *J. Biol. Chem. 255*, 9082−9092.
16. Parry, R. J., and Minta, A. (1982) *J. Am. Chem. Soc. 104*, 871−872.
17. Markham, G. D., Parkin, D. W., Mentch, F., and Schramm, V. L. (1987) *J. Biol. Chem. 262*, 5609−5615.
18. Ma, Q.-F., Kenyon, G. L., and Markham, G. D. (1990) *Biochemistry 29*, 1412−1416.
19. McQueney, M. S., and Markham, G. D. (1995) *J. Biol. Chem. 270*, 18277−18284.
20. Reczkowski, R. S., Taylor, J. C., and Markham, G. D. (1998) *Biochemistry 37*, 13499−13506.
21. Reczkowski, R. S., and Markham, G. D (1999) *Biochemistry 38*, 9063−9068.
22. Taylor, J. C., and Markham, G. D. (1999) *J. Biol. Chem. 274*, 32909−32914.
23. Takusagawa, F., Kamitori, S., and Markham, G. D. (1996) *Biochemistry 35*, 2586−2596.
24. Takusagawa, F., Kamitori, S., Misaki, S., and Markham, G. D. (1996) *J. Biol. Chem. 271*, 136−147.
25. Fu, Z., Hu, Y., Markham, G. D., and Takusagawa, F. (1996) *J. Biomol. Struct. Dyn. 13*, 727−739.
26. Anderson, K. S., and Johnson, K. A. (1990) *Chem. Rev. 90*, 1131−1149.
27. Johnson, K. A. (1992) in *The Enzymes*, Vol. 20, pp 1−62, Academic Press, New York.
28. Cohn, M. (1992) *Annu. Rev. Biophys. Biomol. Struct. 21*, 1−24.
29. Boyer, P. D. (1978) *Acc. Chem. Res. 11*, 218−224.
30. Rose, I. A. (1995) *Methods Enzymol. 249*, 315−340.
31. Sufrin, J. R., Lombardini, J. B., and Keith, D. D. (1982) *Biochem. Biophys. Res. Commun. 106*, 251−255.
32. Glazer, R. I., and Peale, A. L. (1978) *Anal. Biochem. 91*, 516−520.
33. Dunaway-Mariano, D., and Cleland, W. W. (1980) *Biochemistry 19*, 1496−1505.
34. Mertens, M. L., and Kägi, J. H. R. (1979) *Anal. Biochem. 96*, 448−455.
35. Ward, L. D. (1985) *Methods Enzymol. 117*, 400−414.
36. Wilkinson, K. D., and Rose, I. A. (1979) *J. Biol. Chem. 254*, 12567−12572.
37. Rose, I. A. (1980) *Methods Enzymol. 64*, 47−59.
38. Bochner, B. R., and Ames, B. N. (1982) *J. Biol. Chem. 257*, 9759−9769.

39. Cohn, M., and Hu, A. (1978) *Proc. Natl. Acad. Sci. U.S.A. 75*, 200−203.
40. Barshop, B. A., Wrenn, R. F, and Frieden, C. (1983) *Anal. Biochem. 130*, 134−145.
41. Zimmerle, C. T., and Frieden, C. (1989) *Biochem. J. 258*, 381−387.
42. Anderson, K. S., Sikorski, J. A., and Johnson, K. A. (1988) *Biochemistry 27*, 7395−7406.
43. Saint-Girons, I., Parsot, C., Zakin, M. M., Barzu, O., and Cohen, G. N. (1988) *Crit. Rev. Biochem. 23*, S1−S42.
44. Kotb, M., and Kredich, N. M. (1985) *J. Biol. Chem. 260*, 3923−3930.
45. Chiang, P. K., and Cantoni, G. L. (1977) *J. Biol. Chem. 252*, 4506−4513.
46. Hackney, D. D. (1980) *J. Biol. Chem. 255*, 5320−5328.
47. Kukko-Kalske, E., Lintunen, M., Inen, M. K., Lahti, R., and Heinonen, J. (1989) *J. Bacteriol. 171*, 4498−4500.
48. Albe, K. R., Butler, M. H., and Wright, B. E. (1990) *J. Theor. Biol. 143*, 163−195.
49. Knowles, J. R. (1991) *Nature 350*, 121−124.
50. Fersht, A. (1999) *Structure and Mechanism in Protein Science*, Freeman, New York.
51. Smirnova, I. N., Kasho, V. N., Volk, S. E., Ivanov, A. H., and Baykov, A. A. (1995) *Arch. Biochem. Biophys. 318*, 340−348.
52. Taylor, J. C., Takusagawa, F., and Markham, G. D. (1996) *FASEB J. 10*, A970.
53. Perez-Mato, I., Castro, C., Ruiz, F. A., Corrales, F. J., and Mato, J. M. (1999) *J. Biol. Chem. 274*, 17075−17079.

BI992876S